UDC 53.088:62 – 754.2 (045)
V. Apostolyuk

CROSS-COUPLING COMPENSATION FOR CORIOLIS VIBRATORY GYROSCOPES

Introduction

Many modern angular rate sensors operate using sensing of the Coriolis force induced motion in vibrating structures. Such approach allows to avoid using expensive means of mechanisation as well as to increase long term reliability of sensors. Another benefit lays in the possibility to fabricate sensitive elements of such gyroscopes in miniature form by using modern microelectronic mass-production technologies. Such gyroscopes are frequently referred to as MEMS (Micro-Electro-Mechanical-Systems) gyroscopes.

An important performance parameter for a vibratory gyroscope is its zero rate output or zero bias. Geometrical imperfections in the vibrating mechanical structure and/or the sense and drive electrodes as well as electrical coupling between these electrodes can cause an output signal in the absence of rotation [1]. Specifically for shell gyroscope designs, cross-damping of the vibrating structure can also cause a rate-like output when there is no rotation [2].

In view of these problems, development of the efficient decoupling system for Coriolis vibratory gyroscopes (CVG) is highly necessary.

This paper demonstrates synthesis of such a decoupling system, that allows either partial or complete removal of the undesired cross-couplings both for cross-stiffness and cross-damping.

Problem formulation

In order to solve the problem of undesired cross-coupling compensation for CVGs, we have to determine structure of the decoupling loop and identify its transfer functions. Performance of the obtained decoupling system will be verified using numerical simulations.

Coupled motion equations of CVG

In the most generalized form, motion equations of the CVG sensitive element both with translational and rotational motion could be represented in the following form [3]:

$$\begin{cases} \ddot{x}_1 + 2\zeta_1 k_1 \dot{x}_1 + (k_1^2 - d_1\Omega^2)x_1 + g_1\Omega\dot{x}_2 + d_3\dot{\Omega}x_2 = q_1(t), \\ \ddot{x}_2 + 2\zeta_2 k_2 \dot{x}_2 + (k_2^2 - d_2\Omega^2)x_2 - g_2\Omega\dot{x}_1 - \dot{\Omega}x_1 = q_2(t). \end{cases} \quad (1)$$

Here x_1 and x_2 are the generalized coordinates that describe primary (excited) and secondary (sensed) motions of the sensitive element respectively, k_1 and k_2 are the corresponding natural frequencies, ζ_1 and ζ_2 are the dimensionless relative damping coefficients, Ω is the measured angular rate, which is orthogonal to the axes of primary and secondary motions, q_1 and q_2 are the generalized accelerations due to the external forces acting on the sensitive element. The remaining dimensionless coefficients are different for the sensitive elements exploiting either translational or rotational motion. For the translational sensitive element they are $d_1 = d_2 = 1$, $d_3 = m_2/(m_1 + m_2)$, $g_1 = 2m_2/(m_1 + m_2)$, $g_2 = 2$, where were m_1 and m_2 are the masses of the outer frame and the internal massive element. In case of the rotational motion of the sensitive element, these coefficients are the functions of different moments of inertia (for greater details see [4]).

Equations (1) are coupled by the angular rate terms, which results in the fundamental capability of such a system to measure external rotation. However, in a more realistic system other cross-coupling will be present, manifesting itself as a cross-damping and cross-stiffness. Assuming small and quasi-constant angular rate ($\Omega^2 \approx 0$ and $\dot{\Omega} \approx 0$), incorporating cross-coupling terms, sensitive element motion equations will then be

$$\begin{cases} \ddot{x}_1 + 2\zeta_1 k_1 \dot{x}_1 + k_1^2 x_1 = q_1(t) - g_1 \Omega \dot{x}_2 - d_{12}\dot{x}_2 - c_{12} x_2, \\ \ddot{x}_2 + 2\zeta_2 k_2 \dot{x}_2 + k_2^2 x_2 = q_2(t) + g_2 \Omega \dot{x}_1 + d_{21}\dot{x}_1 + c_{21} x_1, \end{cases} \tag{2}$$

were d_{12} and d_{21} are the undesired cross-damping coefficients, c_{12} and c_{21} are the undesired cross-stiffness coefficients. These cross-coupling coefficients must by compensated, while the crucial term with the angular rate must be preserved.

Sensitive element structural diagram

By applying Laplace transformation to both sides of the system (2) with respect to zero initial conditions, we can obtain

$$\begin{cases} (s^2 + 2\zeta_1 k_1 s + k_1^2) x_1(s) = q_1(s) - (g_1 \Omega s + d_{12} s + c_{12}) x_2(s), \\ (s^2 + 2\zeta_2 k_2 s + k_2^2) x_2(s) = q_2(s) + (g_2 \Omega s + d_{21} s + c_{21}) x_1(s). \end{cases} \tag{3}$$

Sensitive element of CVG as an element of control systems and governed by the equations (3) can be represented by means of the structural scheme shown in Fig. 1 ([4, 5]).

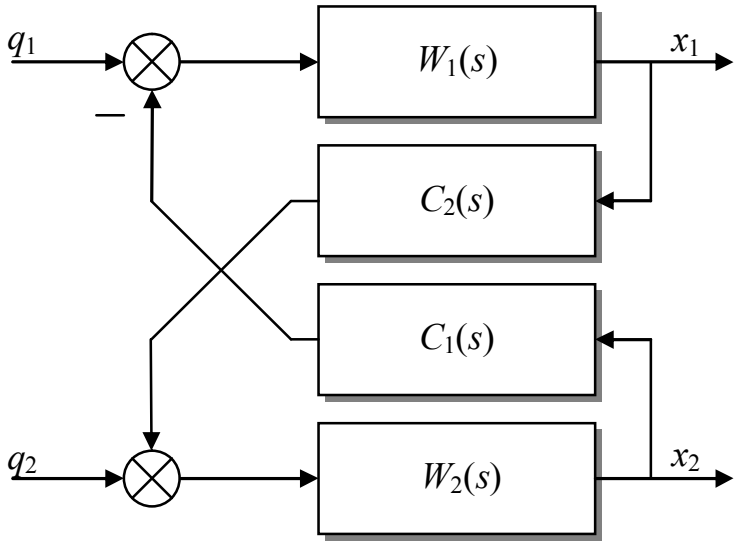

Fig. 1. Structural diagram of CVG

Transfer functions in Fig. 1 are defined as

$$\begin{aligned} W_1(s) &= \frac{1}{s^2 + 2\zeta_1 k_1 s + k_1^2}, \\ W_2(s) &= \frac{1}{s^2 + 2\zeta_2 k_2 s + k_2^2}, \\ C_1(s) &= (g_1\Omega + d_{12})s + c_{12}, \\ C_2(s) &= (g_2\Omega + d_{21})s + c_{21}. \end{aligned} \tag{3}$$

For this system its outputs can be found from the following system of algebraic equations:

$$\begin{cases} x_1(s) = W_1(s)[q_1(s) - C_1(s)x_2(s)], \\ x_2(s) = W_2(s)[q_2(s) + C_2(s)x_1(s)]. \end{cases} \tag{4}$$

Thus, solving system (4) and omitting Laplace variable "s" one can find outputs of the CVG:

$$\begin{aligned} x_1 &= \frac{W_1}{1 + C_1 C_2 W_1 W_2} q_1 - \frac{C_1 W_1 W_2}{1 + C_1 C_2 W_1 W_2} q_2, \\ x_2 &= \frac{W_2}{1 + C_1 C_2 W_1 W_2} q_2 + \frac{C_2 W_1 W_2}{1 + C_1 C_2 W_1 W_2} q_1. \end{aligned} \tag{5}$$

One should note, that in an ideal case of only useful Coriolis cross-coupling present in the system

$$\begin{aligned} C_1(s) &\to C_{10}(s) = g_1\Omega s, \\ C_2(s) &\to C_{20}(s) = g_2\Omega s. \end{aligned} \tag{6}$$

Similarly, ideal system outputs can be obtained by substituting expressions (6) into expressions (5).

Decoupling system synthesis

Let us consider the structure shown in Fig. 2 that is added to the outputs of the CVG sensitive element as shown in Fig. 1. Here transfer functions H_1, H_2, G_1, and G_2 are unknown and yet to be determined. Outputs of this system can be calculated as

$$\begin{aligned} y_1(s) &= H_1(s)x_1(s) + G_1(s)x_2(s), \\ y_2(s) &= H_2(s)x_2(s) - G_2(s)x_1(s). \end{aligned} \tag{7}$$

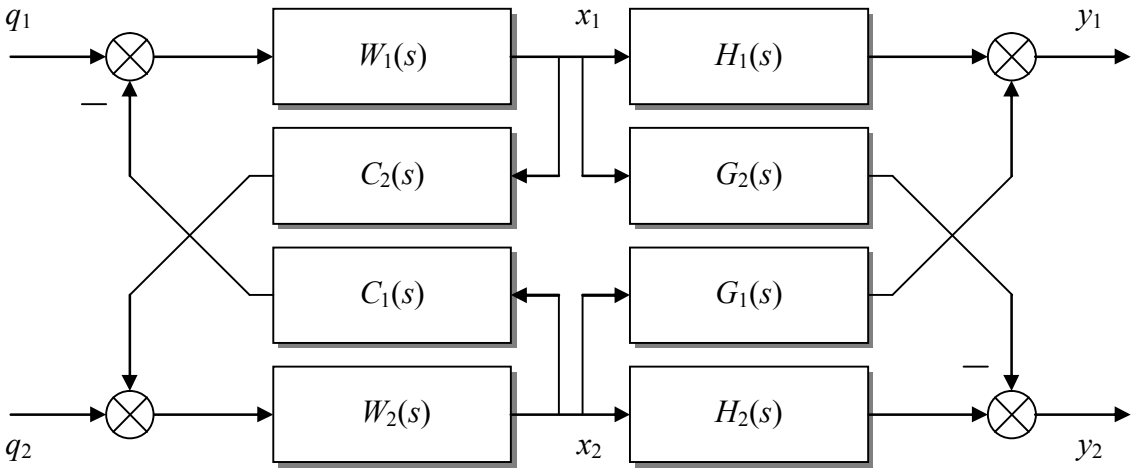

Fig. 2. CVG with the decoupling structure

Substituting (5) into (7) yields

$$\begin{aligned} y_1 &= \frac{H_1W_1 + C_2G_1W_1W_2}{1 + C_1C_2W_1W_2}q_1 + \frac{G_1W_2 - C_1H_1W_1W_2}{1 + C_1C_2W_1W_2}q_2, \\ y_2 &= \frac{H_2W_2 + C_1G_2W_1W_2}{1 + C_1C_2W_1W_2}q_2 - \frac{G_2W_1 - C_2H_2W_1W_2}{1 + C_1C_2W_1W_2}q_1. \end{aligned} \tag{8}$$

Assuming that outputs (8) after the decoupler must be identical to ideal system output, and comparing the corresponding transfer functions (coefficients of q_1 and q_2), the following system of equation can be produced:

$$\begin{cases} \dfrac{H_1W_1 + C_2G_1W_1W_2}{1 + C_1C_2W_1W_2} = \dfrac{W_1}{1 + C_{10}C_{20}W_1W_2}, \\ \dfrac{G_1W_2 - C_1H_1W_1W_2}{1 + C_1C_2W_1W_2} = -\dfrac{C_{10}W_1W_2}{1 + C_{10}C_{20}W_1W_2}, \\ \dfrac{H_2W_2 + C_1G_2W_1W_2}{1 + C_1C_2W_1W_2} = \dfrac{W_2}{1 + C_{10}C_{20}W_1W_2}, \\ -\dfrac{G_2W_1 - C_2H_2W_1W_2}{1 + C_1C_2W_1W_2} = \dfrac{C_{20}W_1W_2}{1 + C_{10}C_{20}W_1W_2}. \end{cases} \tag{9}$$

System (9) can now be solved for unknown transfer functions H_1, H_2, G_1, and G_2, resulting in

$$\begin{aligned} G_1 &= \frac{(C_1 - C_{10})W_1}{1 + C_{10}C_{20}W_1W_2}, \; G_2 = \frac{(C_2 - C_{20})W_2}{1 + C_{10}C_{20}W_1W_2}, \\ H_1 &= \frac{1 + C_{10}C_2W_1W_2}{1 + C_{10}C_{20}W_1W_2}, \; H_2 = \frac{1 + C_{20}C_1W_1W_2}{1 + C_{10}C_{20}W_1W_2}. \end{aligned} \tag{10}$$

Finally, substituting expressions (3) and (6) into solutions (10) results in the CVG decoupling system transfer functions:

$$\begin{aligned} G_1(s) &= \frac{(c_{12} + d_{12}s)(s^2 + 2\zeta_2k_2s + k_2^2)}{\Delta(s)}, \\ G_2(s) &= \frac{(c_{21} + d_{21}s)(s^2 + 2\zeta_1k_1s + k_1^2)}{\Delta(s)}, \\ H_1(s) &= 1 + \frac{g_1s(c_{21} + d_{21}s)}{\Delta(s)}\Omega, \\ H_2(s) &= 1 + \frac{g_2s(c_{12} + d_{12}s)}{\Delta(s)}\Omega, \\ \Delta(s) &= (s^2 + 2\zeta_1k_1s + k_1^2)(s^2 + 2\zeta_2k_2s + k_2^2) + g_1g_2s^2\Omega^2. \end{aligned} \tag{11}$$

Since it has been already assumed that angular rate Ω is small (e.g. $\Omega^2 \approx 0$), expressions (11) can be further simplified as

$$\begin{aligned} G_1(s) &= \frac{c_{12} + d_{12}s}{s^2 + 2\zeta_1k_1s + k_1^2}, \; G_2(s) = \frac{c_{21} + d_{21}s}{s^2 + 2\zeta_2k_2s + k_2^2}, \\ H_1(s) &= 1 + \frac{g_1s(c_{21} + d_{21}s)}{(s^2 + 2\zeta_1k_1s + k_1^2)(s^2 + 2\zeta_2k_2s + k_2^2)}\Omega, \\ H_2(s) &= 1 + \frac{g_2s(c_{12} + d_{12}s)}{(s^2 + 2\zeta_1k_1s + k_1^2)(s^2 + 2\zeta_2k_2s + k_2^2)}\Omega. \end{aligned} \tag{12}$$

Analysis of the expressions (11) and (12) reveals well expected fact, that if all undesired cross-couplings, such as damping and stiffness, are absent, then these transfer functions are reduced to $G_1 = G_2 = 0$, $H_1 = H_2 = 1$. However, one could also note, that these transfer functions depend on the unknown angular rate Ω.

Partial decoupling system

Taking into consideration the fact, that secondary oscillations are usually significantly smaller than primary oscillations, it is justifiable to assume that influence of secondary oscillations on primary is negligibly small. Besides, only secondary oscillations output is used to measure angular rate. Hence, decoupling structure can be simplified as shown in Fig. 3.

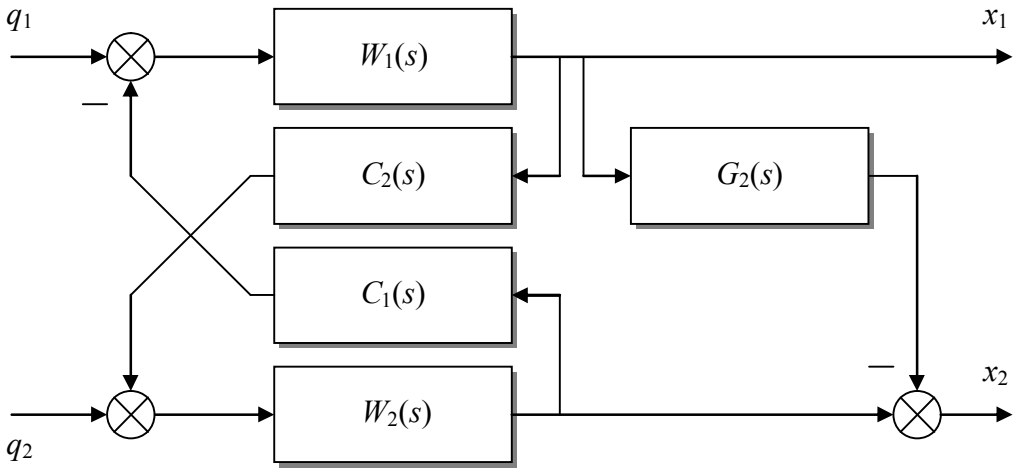

Fig. 3. CVG with the partial decoupling system

Here transfer function G_2 is given by (12). Important feature of the system shown in Fig. 3 is that it doesn't depend on angular rate. Let us evaluate the performance of this system by means of numerical simulation. Measured angular rate with and without partial decoupling system is shown in Fig. 4.

Here $d_{12} = -d_{21} = 0.5$, $c_{12} = c_{21} = 50000$. One can see that even partial decoupling system significantly improves performance of CVG.

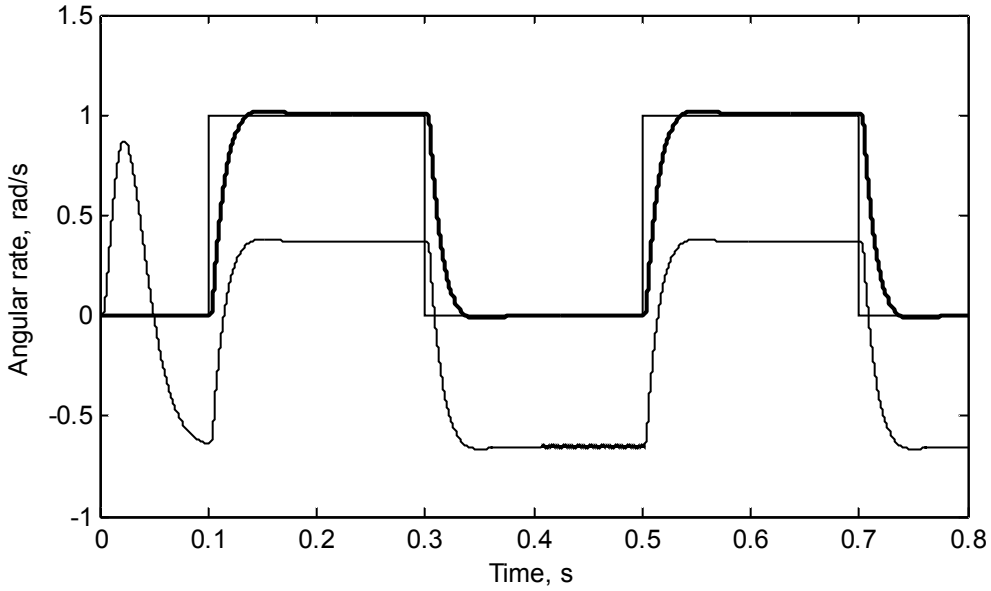

Fig. 4. Results of numerical simulations
(dotted – input angular rate, dashed – without decoupling, solid – with decoupling)

Linearised complete decoupling system

Although considered above partial decoupling system somewhat decouples CVG from undesired couplings, it is still might not be sufficient for the high performance devices. At the same time, complete decoupling system based upon transfer functions (11) is not feasible due to the presence of the unknown angular rate as a coefficient in its transfer functions. However, in the linearised expressions (12) angular rate is present only as an additional input to the decoupling system. Such peculiarity allows to build decoupling system by means of feeding decoupled angular rate back to the decoupling system, as shown in Fig. 5.

Here, in Fig. 5, block "CVG Sensitive Element" has been already shown in Fig 1, block "Secondary Demodulator" demodulates secondary oscillations and produces measured angular rate as its output. Finally, feedback transfer function $H_{20}(s)$ is given by the following expression:

$$H_{20}(s) = \frac{g_2 s(c_{12} + d_{12} s)}{(s^2 + 2\zeta_1 k_1 s + k_1^2)(s^2 + 2\zeta_2 k_2 s + k_2^2)}. \tag{13}$$

Expression (13) is determined directly from (12) as a coefficient to the angular rate in the expression for the transfer function $H_2(s)$.

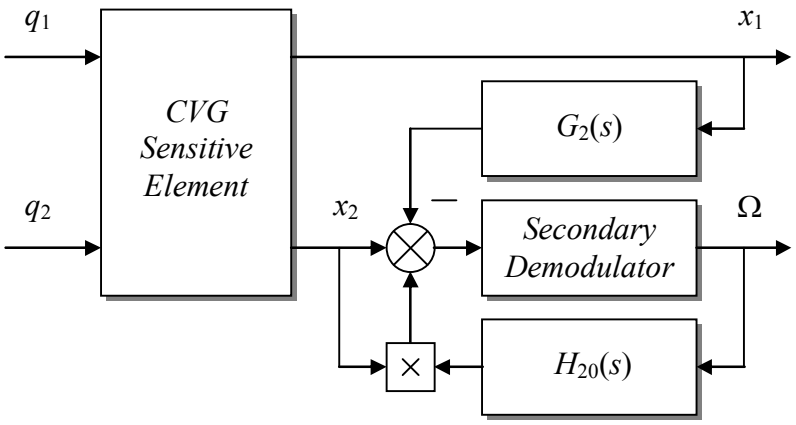

Fig. 5. Linearised complete decoupling system

In order to evaluate performance of the linearised decoupling system in comparison with the partial decoupling system, let us numerically simulate operation of a realistic CVG with these two systems. Essential part of a unit step transient processes is shown in Fig. 6.

Although the presented in Fig. 5 system is non-linear, its performance is apparently better than performance of the partial decoupling system.

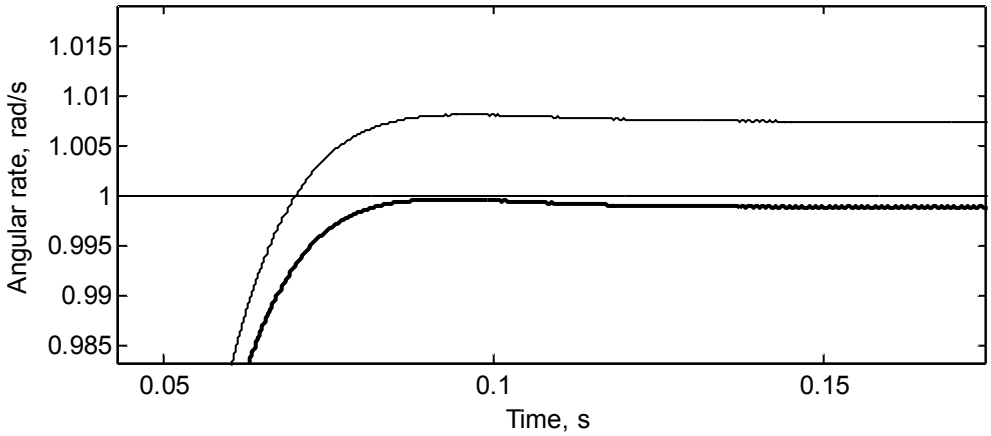

Fig. 6. Decoupling systems performance comparison
(dotted – input angular rate, dashed – partial decoupler, solid – linearised complete decoupler)

Conclusions

Proposed in the paper structure and transfer function synthesis allow considerable improvement of the CVG performances by means of practical elimination of undesired cross-couplings. Partial decoupling system is suggested for the devices with low accuracy requirements due to its simplicity. For the high

performance sensors usage of the linearised complete decoupling system can be justified. Both these approaches improve bias and scale factor stability of CVG.

However, in order to efficiently utilise such decoupling systems, one should first identify parameters of the undesired cross-couplings. Problem of identifying these parameters is therefore views as a logical continuation to the presented above research.

References

1. *Yazdi N., Ayazi F., Najafi K.* Micromachined Intertial Sensors // Proceedings of the IEEE, Vol. 86, No. 8, 1998, pp. 1640-1659.
2. *Chikovani V.V., Umakhanov E.O., Marusyk P.I.* The Compensated Differential CVG // Proceedings Symposium Gyro Technology 2008, Karlsruhe, Germany, pp. 3.1-3.8.
3. *Apostolyuk V. A.* Theory and Design of Micromechanical Vibratory Gyroscopes // MEMS/NEMS Handbook (Ed: Cornelius T. Leondes), Springer, 2006, Vol.1, Chapter 6, pp. 173-195.
4. *Apostolyuk V., Tay F.* Dynamics of Micromechanical Coriolis Vibratory Gyroscopes // Sensor Letters, Vol. 2, No. 3-4, 2004, pp. 252-259.
5. *Apostolyuk V.A.* Dynamics of Coriolis Vibratory Gyroscopes in Control Systems // Systems of Control, Navigation, and Communication, No. 1 (13), 2010, pp. 62-66.